



## Carbon coating of $\text{Li}_4\text{Ti}_5\text{O}_{12}$ using amphiphilic carbonaceous material for improvement of lithium-ion battery performance

Xuefei Guo, Chengyang Wang\*, Mingming Chen, Jiuzhou Wang, Jiaming Zheng

Key Laboratory for Green Chemical Technology of Ministry of Education, School of Chemical Engineering and Technology, Tianjin University, Tianjin 300072, China

### HIGHLIGHTS

- ▶ Carbon-coated  $\text{Li}_4\text{Ti}_5\text{O}_{12}$  was prepared by using ACM as a carbon precursor.
- ▶ The obtained  $\text{Li}_4\text{Ti}_5\text{O}_{12}$  electrode presents high-rate capability and cyclic stability.
- ▶ This economic, facile, and green synthesis method enables the production on a large scale.

### ARTICLE INFO

#### Article history:

Received 14 March 2012  
Received in revised form  
27 April 2012  
Accepted 29 April 2012  
Available online 3 May 2012

#### Keywords:

Lithium titanate  
Amphiphilic carbonaceous material  
Anode material  
Lithium-ion batteries

### ABSTRACT

Carbon coating of fine particles of  $\text{Li}_4\text{Ti}_5\text{O}_{12}$  synthesized under hydrothermal condition is carried out by amphiphilic carbonaceous material (ACM) in aqueous solution, followed by carbonization at  $800^\circ\text{C}$  for 2 h. The particles prepared are comprised of highly-crystalline spinel-type  $\text{Li}_4\text{Ti}_5\text{O}_{12}$  with the size in the range of 100–400 nm without any agglomeration, of which surface is uniformly covered by a thin carbon layer. Their electrochemical performance as an anode in lithium-ion batteries is evaluated. The initial discharge capacity of carbon-coated  $\text{Li}_4\text{Ti}_5\text{O}_{12}$  at 20 C rate is  $137\text{ mA h g}^{-1}$  and remains as high as  $125\text{ mA h g}^{-1}$  after 100 cycles (91% retention), exhibiting good rate and cyclic performance. Carbon coating by using ACM as carbon precursor gives the  $\text{Li}_4\text{Ti}_5\text{O}_{12}$  particles an enhanced performance as an anode in lithium-ion batteries, owing to the improvement in electrical conductivity, polarization and ability of dispersion. This non-organic coating process may present a new economic, facile, and green pathway for the preparation of carbon-coated  $\text{Li}_4\text{Ti}_5\text{O}_{12}$  as a high power anode material in lithium-ion batteries.

© 2012 Elsevier B.V. All rights reserved.

### 1. Introduction

Energy storage is an important problem to realize low carbon society and there have been carried out many challenges [1]. Li-ion batteries (LIBs) have been widely used for portable electric devices, such as mobile phones and notebooks. However, the performance of today's commercial LIBs still cannot meet the requirements of some industrial applications, such as in electric vehicles and sustainable energy storage, in terms of high power density, long cycle life and high safety [2–4].

The spinel-type lithium titanate ( $\text{Li}_4\text{Ti}_5\text{O}_{12}$ , LTO) has attracted great interest as anode material of rechargeable lithium-ion batteries because of its unique characteristics: (1) zero strain during charging and discharging, (2) excellent cycle reversibility, (3) fast  $\text{Li}^+$  insertion and de-insertion ability and (4) high lithiation

voltage plateau at 1.55 V vs.  $\text{Li}/\text{Li}^+$ , which sufficiently avoid the formation of metallic lithium, therefore improving the safety of Li-ion batteries [5–8]. All of these merits make  $\text{Li}_4\text{Ti}_5\text{O}_{12}$  more competitive as a safe anode material for long life LIBs. Unfortunately, the high-rate performance of bulk LTO is hindered by its inherent poor electronic conductivity (ca.  $10^{-13}\text{ S cm}^{-1}$ ) and moderate  $\text{Li}^+$  diffusion coefficient ( $10^{-8}\text{ cm}^2\text{ s}^{-1}$ ) [9], which makes the polarization of the electrode serious at the charged/discharged with high current densities. Various research works have focused on developing strategies to overcome this problem, such as reducing particle size [10,11], doping with other metals or metal oxides [12–14], mixing with a conductive second phase [15] and coating with conductive materials [16–19].

Carbon coating of LTO particles is supposed to be the most effective and low cost way, because it improves the surface electronic conductivity and the electrical contact with electrolyte solution, and, in turn, leads to a significantly improved electrochemical performance [20]. However, its effect depends on the amount and the nature of carbon coated. Until now, carbon coating

\* Corresponding author. Tel./fax: +86 22 27890481.  
E-mail address: [cywang@tju.edu.cn](mailto:cywang@tju.edu.cn) (C. Wang).

was mainly carried out by either chemical vapor deposition (CVD) [16] or heat treatment of a mixture with an organic precursor at a high temperature under inert atmosphere [17–19]. Thickness and uniformity of carbon layer is also important factor to get better performance: a non-continuous carbon layer cannot improve the electronic conductivity effectively, while the excessively thick coated layer may restrict the efficient charge transfer/transport [19]. Therefore forming a thin and uniform carbon layer on the LTO surface is critical, in addition to choosing an appropriate carbon precursor to control nature of carbon layer coated.

“Amphiphilic carbonaceous material” (ACM), a kind of water-dispersible carbonaceous material, especially in alkaline aqueous solution, was firstly synthesized from coke by Fujii et al. [21–24], showing that hydrophilic groups, such as  $-\text{COOH}$ ,  $-\text{OH}$  and  $-\text{SO}_3\text{H}$ , existed in ACM make it dispersible in alkaline aqueous solutions in nano-scale. These functional groups may provide a better connection with other material to form a homogenous contact through interfacial interaction on the process to carbon coating. Compared with conventional solid carbon precursors, the ACM aqueous solution is more favorable for forming a thin uniform layer on the particle surface. In our previous work, artificial graphite powder was coated by carbon via an ACM aqueous solution, enhancing its electrochemical performance as electrode in lithium batteries [25].

In this work,  $\text{Li}_4\text{Ti}_5\text{O}_{12}$  synthesized via a hydrothermal method was coated with ACM in its aqueous solution, by expecting a marked improvement in anode performance in LIBs, similar to the case of graphite [25]. The high-rate performances of the carbon-coated LTO in LIBs were investigated by galvanostatic charge/discharge tests, cyclic voltammetry and electrochemical impedance spectroscopy.

## 2. Experimental

### 2.1. Synthesis

The spinel  $\text{Li}_4\text{Ti}_5\text{O}_{12}$  was synthesized under a hydrothermal condition.  $\text{LiOH}$  solution was added in dropwise to 0.5 M  $\text{TiCl}_4$  aqueous solution with stirring at room temperature in stoichiometric ratio, and then the mixture was transferred into a Teflon-lined stainless steel autoclave, sealed and maintained at 170 °C for 24 h. The precipitate was collected by centrifugation, thoroughly washed three times in distilled water and three times in ethanol to the neutral condition, and then dried in a vacuum at 100 °C. Subsequently, LTO was obtained white powder after calcination at 800 °C for 6 h in air. ACM was prepared from a green needle coke having high carbon content, low volatile and ash contents, according to the procedure reported in earlier reports [26].

Carbon coating of LTO was performed as follows: 1 g of LTO was dispersed in an aqueous solution with different amounts (50, 80 and 100 mg) of ACM in 100 ml water, stirred for 3 h at 80 °C, recovered by the evaporation of water, and then heat-treated at 800 °C for 2 h in nitrogen atmosphere to carbonize ACM. The resulting carbon-coated LTO samples were named as shown in Table 1, together with the pristine LTO.

### 2.2. Physical characterization

Power X-ray diffraction (XRD) measurement was carried out using a Rigaku D/max 2500v/PC system using  $\text{Cu K}\alpha$  radiation ( $\lambda=1.5406 \text{ \AA}$ ). Raman spectrum was measured by a Renishaw in Via Raman microscope at room temperature with the 532 nm line of an Ar ion laser as an excitation source. Thermogravimetric analysis (TG) was run on a TA-50 instrument up to 800 °C under air to determine the carbon content of the sample. Morphology and structure of the samples were analyzed via field-emission scanning

**Table 1**  
Preparation condition and carbon content of the samples.

Sample code	ACM used (mg/g of LTO)	ACM content after drying (mass%) <sup>a</sup>	Carbon content after calcinations (mass%)	Lattice parameters of LTO (nm)
LTO	0	0.0	0.00	0.8358
LTO/C-5	50	4.8	2.6	0.8358
LTO/C-8	80	7.4	4.4	0.8359
LTO/C-10	100	9.1	5.7	0.8359

<sup>a</sup> The ACM content is calculated by the amount of ACM divided by the total mass.

electron microscopy (FE-SEM, S4800, ThermoFisher) and high-resolution transmission electron microscopy (HR-TEM, Tecnai G2F20, Philips). The particle size and distribution were obtained using a laser granulometer (Zetasizer Nano S90, Malvern).

### 2.3. Electrochemical characterizations

The electrochemical measurements were performed using CR2032 coin-type cells. The slurry, which was prepared by mixing the sample powder (active material), acetylene black, and poly(vinylidene fluoride) (PVDF) binder in a weight ratio of 80:10:10 in an N-methyl-2-pyrrolidone (NMP) solution, was uniformly pasted onto Cu foil and then dried at 120 °C in a vacuum oven to construct electrode sheet. In the cell lithium metal was used as the counter electrode, porous polypropylene film as the separator, and 1.0 M  $\text{LiPF}_6$  in the mixture of ethylene carbonate and diethyl carbonate (EC/DEC, 1:1, v/v) as the electrolyte. The cyclic voltammogram was recorded from 1.0 to 3.0 V vs.  $\text{Li/Li}^+$  at different scanning rates ranging from 0.1 to 10  $\text{mV s}^{-1}$  using a Princeton Parstant 2273 electrochemical system. The galvanostatic charge/discharge was performed on a Land BT2000 battery test system (Wuhan, P.R. China) with different current densities of 0.1–20 C (1C means insertion of 3 mol  $\text{Li}^+$  into LTO in 1 h, i.e., 175  $\text{mA g}^{-1}$  in the present cell) and cycled up to 100th. In this cell charging is the insertion of  $\text{Li}^+$  into the host LTO and discharging is the extraction  $\text{Li}^+$  from the host, and are carried out by using the same current density. Capacity of the cell was calculated on the basis of the total mass of the active material (sample). Complex impedance measurements were also carried out using Princeton Parstant 2273 electrochemical system in the frequency range from 10 mHz to 100 kHz with a potential perturbation at 10 mV.

## 3. Results

### 3.1. Structure and morphology

Fig. 1 shows the XRD pattern of the synthesized LTO samples. All the peaks can be indexed, as shown in the figure, on the basis of cubic spinel structure with  $Fd\bar{3}m$  space group and coincide with the powder pattern presented in JCPDS card No. 26-1198, although there are very small peaks due to unknown phases, which are possible to be detected only by enlarging diffraction pattern, being shown as an inset in Fig. 1. The lattice parameter  $a_0$  of the LTO phase is determined as 0.8358 nm (Table 1), which is in accordance with the value 0.8357 nm reported on LTO, suggesting that the existence of ACM gives no appreciable effect on the crystalline phase of LTO during heat treatment. The carbon content in the sample after carbonization depends on the amount of ACM used, from 2.6 to 5.7 mass%, as shown in Table 1. The carbon formed by the carbonization at 800 °C was supposed to be amorphous structure and also in low content, so that no diffraction peak of carbon was detected (Fig. 1). On Raman spectrum, broad G- and D-bands due to carbon [27] are clearly observed on the carbon-coated LTO samples, although the pristine LTO does not show any peak around this

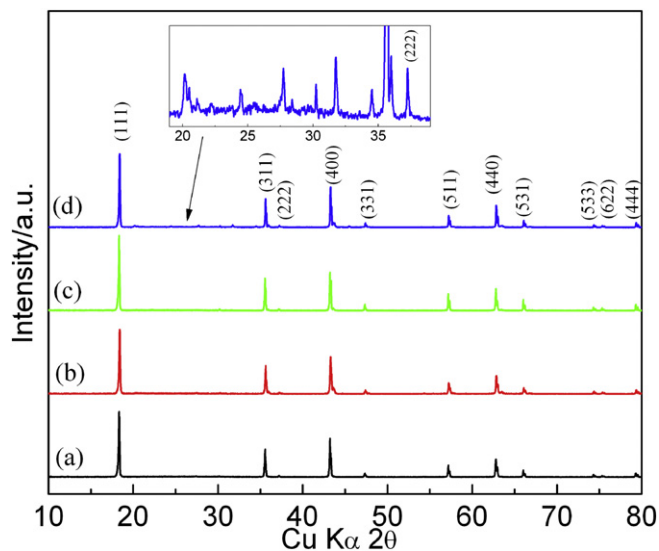


**Fig. 1.** X-ray diffraction patterns of pristine LTO, (b) LTO/C-5, (c) LTO/C-8 and (d) LTO/C-10.

Raman shift, evidencing the presence of amorphous carbon in the carbon-coated LTO.

LTO particles changed their color from white to brown without noticeable aggregation after coating of ACM and then to black after

the carbonization at 800 °C, because ACM was converted into carbon. The powders looked black even under an optical microscope, revealing all LTO particles were coated by carbon.

SEM image in Fig. 2(a) clearly demonstrates that the particles of the pristine LTO have homogenous size in a narrow distribution of about 100–400 nm with minimal agglomeration. It is evident that the hydrothermal method could significantly decrease the particle size of LTO and make the degree of particle agglomeration low, which are supposed to be advantageous for the kinetics of lithium insertion/extraction into the LTO host structure. As shown in Fig. 2(b)–(d), the particles keep almost the same size as that of the pristine LTO after carbon coating at 800 °C, but the agglomeration of particles seems to be noticeable with increasing amount of ACM, i.e., increasing carbon content after the carbonization, indicating that too much ACM causes agglomeration of the carbon-coated LTO particles. The particle size is further investigated by a laser granulometer, as demonstrated in an inset figure in each sample. The result is in good agreement with the result of the SEM of the samples.

High-resolution TEM images of the particles of pristine LTO and carbon-coated LTO, LTO/C-10, in Fig. 3(a) and (b) show that LTO particles are well-crystallized, and the particles of LTO/C-10 sample are coated by carbon layer with about 3 nm thickness.

### 3.2. Electrochemical characterization

Fig. 4(a) and (b) shows the cyclic voltammograms (CVs) of the samples with different scan rates ranging from 0.1 to 10 mV s<sup>-1</sup> in

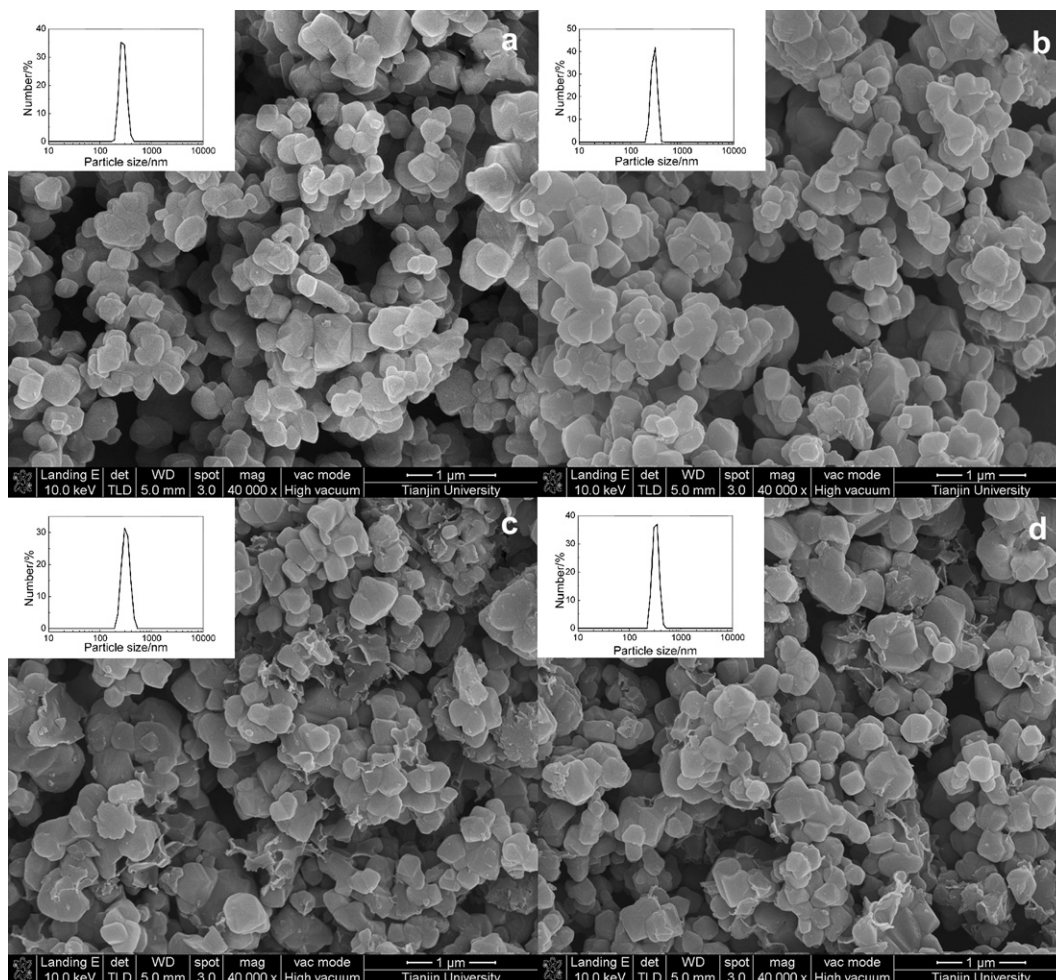


**Fig. 2.** SEM images of (a) pristine LTO, (b) LTO/C-5, (c) LTO/C-8 and (d) LTO/C-10.



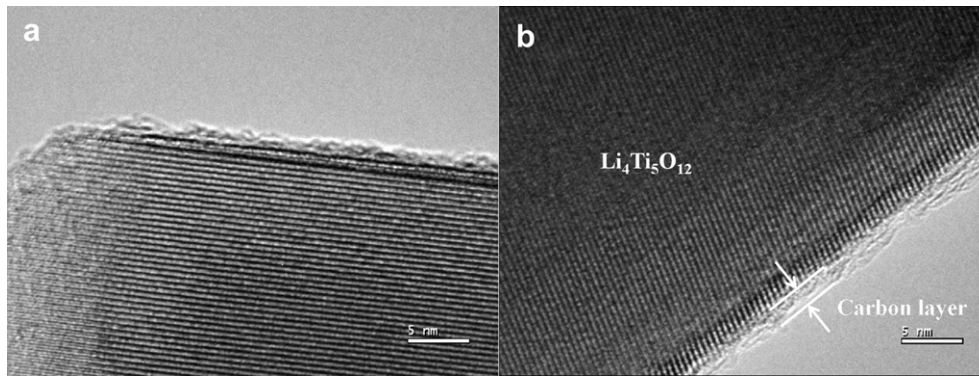


Fig. 3. High-resolution TEM images of (a) pristine LTO and (b) LTO/C-10.

the potential between 1.0 V and 3.0 V. With the slowest scan rate of  $0.1 \text{ mV s}^{-1}$ , a pair of sharp redox peaks is observed on the CV curve at 1.5 V and 1.6 V vs.  $\text{Li}/\text{Li}^+$  for cathodic and anodic scans, respectively, as shown in an inset figure in each sample, which demonstrates the typical behavior of  $\text{Li}^+$  insertion/extraction processes in spinel  $\text{Li}_4\text{Ti}_5\text{O}_{12}$  electrode. The voltage difference between anodic and cathodic peaks can reflect the polarization degree of the electrode: from the comparison in CV shown in Fig. 4, LTO/C-10 consisting of carbon-coated particles has lower polarization compared with the pristine LTO. It can also be seen that the CV curves for the pristine LTO are broadened, particularly on anodic scan, with the increase in scan rate, while those of LTO/C-10 retain a stable shape, showing the weak polarization of the electrode. This suggests an excellent rate capability of the carbon-coated LTO electrodes.

In Fig. 5(a), galvanostatic charge/discharge curves for the sample electrodes in a half-cell at a constant rate of  $0.1\text{C}$  ( $17.5 \text{ mA g}^{-1}$ ) between 1.0 and 3.0 V voltage limits. Both cells show a flat discharge plateau at 1.55 V (vs.  $\text{Li}/\text{Li}^+$ ), which corresponds to the  $\text{Ti}^{3+}/\text{Ti}^{4+}$  redox couple due to Li extraction. The capacity of the platform is about 85–90% of the overall capacity, and the gap between the charge and discharge voltage plateau is very small. Fig. 5(b) and (c) shows the charge/discharge curves of the pristine LTO and LTO/C-10 at different rates from 1C to 20C. With increasing rate, the potential plateau for the pristine LTO becomes shorter and bends down gradually, while that of the carbon-coated LTO remains flat, even though becomes slightly shorter. The gap between the charge and discharge voltage plateau decreases from 0.5 to 0.25 V at 20C, indicating that the polarization decreases by carbon coating and that the rate capability of the carbon-coated LTO electrodes are improved.

In Fig. 5(d) the rate capabilities for the samples are compared in a range of charge/discharge rate from  $0.1\text{C}$  ( $17.5 \text{ mA g}^{-1}$ ) to  $20\text{C}$  ( $3.5 \text{ A g}^{-1}$ ). At a low rate of  $0.1\text{C}$ , discharge capacity for the pristine LTO is  $173 \text{ mA g}^{-1}$ , which is almost the same as usually reported

values [10–19] and close to the theoretical value ( $175 \text{ mA g}^{-1}$ ) [17]. However, those for the carbon-coated LTOs at  $0.1\text{C}$  rate are slightly higher than the pristine LTO, as shown in Fig. 5(a), for example LTO/C-10 giving  $180 \text{ mA g}^{-1}$ . Discharge capacity for the pristine LTO drops significantly with increasing discharge rate, down to  $102 \text{ mA g}^{-1}$  at 20C (58% retention of 1C). While, rate capability for the carbon-coated LTOs becomes much better with increasing carbon content; in particular, LTO/C-10 containing ca. 6 mass% carbon shows an outstanding rate performance delivering discharge capacity as high as  $160 \text{ mA g}^{-1}$  at 10C and  $143 \text{ mA g}^{-1}$  at 20C, 88 and 78% retention of 1C, respectively.

The cycle performance for the carbon-coated LTO, LTO/C-10, at different rates of 1C, 5C and 20C is shown in Fig. 6. Relatively stable cycling is possible. Discharge capacity even after 100 cycles retains 96% of that of the first cycle with 1C, 95% with 5C and 91% with 20C. In particular, cycling stability with 20C is excellent.

AC impedance spectra for the pristine LTO and LTO/C-10 are shown in Fig. 7, together with a simple equivalent circuit. The charge-transfer resistance was calculated from the semicircle in the high-middle frequency range as about  $40 \Omega$  and  $15 \Omega$  for the pristine LTO and LTO/C-10, respectively, suggesting that charge transfer from the electrolyte to active materials LTO is pronouncedly accelerated by the presence of carbon layer at the interface between LTO and electrolyte. However, lithium-ion diffusion process within LTO particle estimated from the oblique line at low frequencies is not influenced by carbon coating.

## 4. Discussion

### 4.1. Carbon coating by using ACM

Carbon coating of LTO particles was successfully performed through immersion in an aqueous solution dispersed ACM nanoparticles and following carbonization. Carbonization yield of the

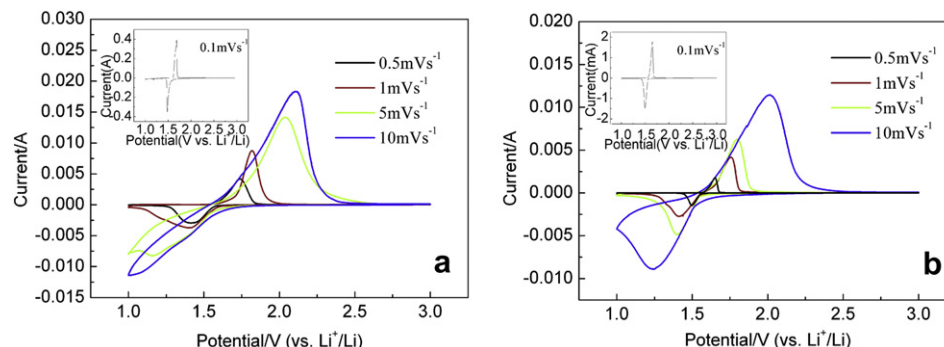
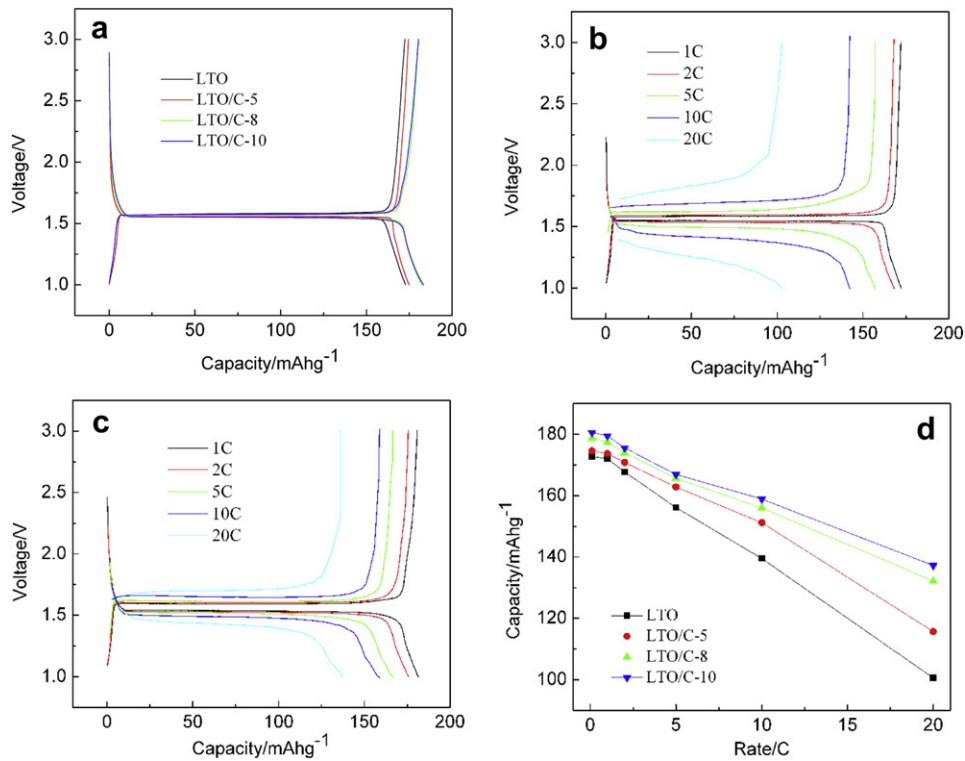


Fig. 4. Cyclic voltammograms of (a) the pristine LTO and (b) LTO/C-10 at scan rates ranging from 0.1 to  $10 \text{ mV s}^{-1}$ .



**Fig. 5.** (a) Charge/discharge curves for the sample electrodes at a rate of 0.1C, Charge/discharge curves for (b) the pristine LTO and for (c) LTO/C-10 with different rates (from 1C to 20C), (d) dependence of specific capacity for the samples on current density.

present ACM is relatively high, as 54–62 mass%, after the carbonization at 800 °C, as expected from the fact that it is derived from a green coke. These experimental results demonstrate that the amount of carbon coating can be easily control by the amount ACM used.

#### 4.2. Battery performance of carbon-coated LTO

Carbon coating improved the rate and cycle performances of LTO particles in LIBs, supposedly due to the enhancement of electrical conductivity and charge transfer at the interface between the active material LTO and electrolyte solution. The increase in capacity with a low rate as 0.1C is not marked because the pristine LTO itself has the capacity close to theoretical one. With a high rate as 20C (3.5 A g<sup>-1</sup>), however, the capacity was markedly enhanced by carbon coating because of the improvement of rate performance. LTO/C-10 coated by about 6 mass% carbon gives discharge capacity of 137 mA g<sup>-1</sup>.

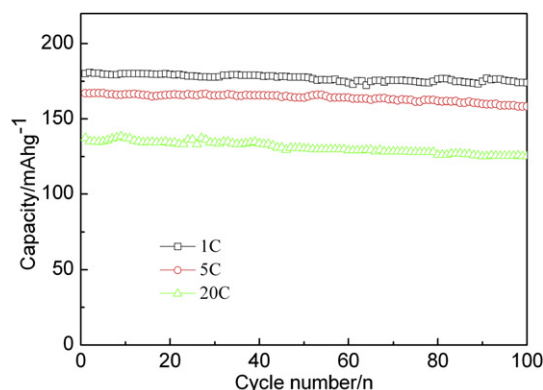


**Fig. 6.** Cycling performance for pristine LTO, LTO/C-10 with different rates.

The rate capability of the carbon-coated LTO electrodes is enhanced by increasing the ACM addition, but not linearly; the rate performance of LTO/C-8 contained 4.4 mass% carbon is very close to LTO/C-10 containing 5.7 mass% carbon. Therefore, it is not advisable to improve the electrochemical performance simply by increasing the carbon content. On one hand, too much ACM is useless for coating and aggravates the coagulation of ACM during carbonization. On the other hand, extortionate carbon content would affect the initial columbic efficiency adversely (another important role in the practical application of LIBs) [15].

With a low rate as 0.1C, LTO/C-10 gave the discharge capacity of 180 mA g<sup>-1</sup>, which was a little higher than theoretical capacity. This extra capacity presumed to be mainly associated with the following two reasons: the re-heat treatment improved the crystallinity of the LTO particles, and a small quantity of LTO was reduced by ACM or formed Ti–C bond during the carbonization (some extremely

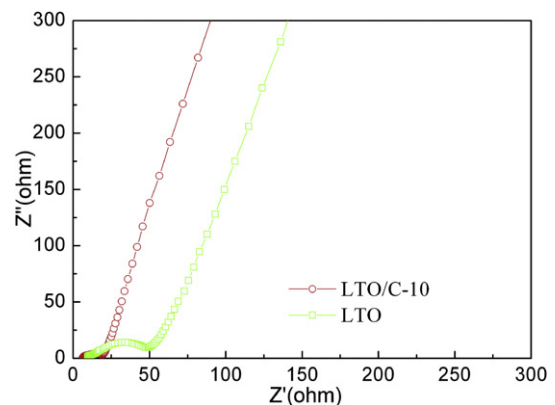


**Fig. 7.** AC impedance spectra for the pristine LTO and LTO/C-10 with an equivalent circuit.

weak unknown peaks have been detected shown in Fig. 1 inset), decreasing the molar mass of the active material or making a different Li-ion insertion mechanism.

## 5. Conclusion

Carbon-coated  $\text{Li}_4\text{Ti}_5\text{O}_{12}$  was prepared by using ACM as a carbon precursor through an organic solvent-free and facile pathway. A reasonable amount of ACM could form a thin uniform coating layer on the LTO particles in the aqueous solution, and after heat treatment, the carbon film obviously improved electrical conductivity, effectively reduced the resistance and polarization of the electrode. As a result, the obtained carbon-coated LTO electrode presents an excellent performance in terms of rate capability, cycling life and capacity retention. This excellent electrochemical performance makes the carbon-coated LTO a promising anode material for high-rate lithium-ion batteries and this economic, facile, and green synthesis method enables its production on a large scale.

## Acknowledgment

This work was financially supported by the Natural Science Foundation of Tianjin City (No. 12JCZDJC27000). And the authors are grateful to Prof. Michio Inagaki at Hokkaido University for helpful suggestions and critical reading of the manuscript.

## References

- [1] M.S. Whittingham, *MRS Bull.* 33 (2008) 411–419.
- [2] B. Scrosati, *Nature* 3 (1995) 73557.
- [3] M. Armand, J.-M. Tarascon, *Nature* 451 (2008) 652.
- [4] K. Zaghib, M. Dontigny, A. Guerfi, P. Charest, I. Rodrigues, A. Mauger, C.M. Julien, *J. Power Sources* 196 (2011) 3949–3954.
- [5] T. Ohzuku, A. Ueda, N. Yamamoto, *J. Electrochem. Soc.* 142 (1995) 1431–1435.
- [6] P.G. Bruce, B. Scrosati, J.M. Tarascon, *Angew. Chem., Int. Ed.* 47 (2008) 2930.
- [7] T.F. Yi, L.J. Jiang, J. Shu, C.B. Yue, R.S. Zhu, H.B. Qiao, *J. Phys. Chem. Solids* 71 (2010) 1236–1242.
- [8] K. Zaghib, M. Simoneau, M. Armand, M. Gauthier, *J. Power Sources* 81–82 (1999) 300.
- [9] C.H. Chen, J.T. Vaughey, A.N. Jansen, D.W. Dees, A.J. Kahaian, T. Goacher, M.M. Thackeray, *J. Electrochem. Soc.* 148 (2001) A102.
- [10] C. Jiang, E. Hosono, M. Ichihara, I. Honma, H. Zhou, *J. Electrochem. Soc.* 155 (2008) A553–A556.
- [11] S.Y. Yin, L. Song, X.Y. Wang, M.F. Zhang, Y.X. Zhang, *Electrochim. Acta* 54 (2009) 5629–5633.
- [12] S. Jia, J. Zhang, W. Wang, Y. Huang, Z. Feng, Z. Zhang, Z. Tang, *Mater. Chem. Phys.* 123 (2010) 510–515.
- [13] A. Sivashanmugam, S. Gopukumar, R. Thirunakaran, C. Nithya, S. Prema, *Mater. Res. Bull.* 46 (2011) 492–500.
- [14] T. Yuan, R. Cai, Z.P. Shao, *J. Phys. Chem. C* 115 (2011) 4943–4952.
- [15] Y. Shi, L. Wen, F. Li, H.M. Cheng, *J. Power Sources* 196 (2011) 8610–8617.
- [16] L. Cheng, X.L. Li, H.J. Liu, H.M. Xiong, P.W. Zhang, Y.Y. Xia, *J. Electrochem. Soc.* 154 (2007) A692–A697.
- [17] H.G. Jung, J. Kim, B. Scrosati, Y.-K. Sun, *J. Power Sources* 196 (2011) 7763–7766.
- [18] L. Yang, L. Gao, *J. Alloys Compd.* 485 (2009) 93–97.
- [19] L. Zhao, Y.S. Hu, H. Li, Z. Wang, L. Chen, *Adv. Mater.* 23 (2011) 1385–1388.
- [20] M. Inagaki, *Carbon* 50 (2012) 3247–3266.
- [21] M. Fujii, Y. Yamada, T. Imamura, in: 18th Biennial Conference of Carbon (1987) pp. 405–408.
- [22] D. Tateishi, K. Esumi, H. Honda, *Carbon* 29 (1991) 1296–1298.
- [23] Z. Li, W. Yan, S. Dai, *Carbon* 42 (2004) 767–770.
- [24] K. Esumi, S. Eshima, Y. Murakami, H. Honda, H. Oda, *Colloids Surf., A* 108 (1996) 113–116.
- [25] J. Wang, M.M. Chen, C.Y. Wang, B. Hu, J.M. Zheng, *Mater. Lett.* 64 (2010) 2281–2283.
- [26] J. Wang, M.M. Chen, C.Y. Wang, J.M. Zheng, in: *Nanoelectronics Conference (INEC) 2010 3rd International* (2010) pp. 222–223.
- [27] W.J. Gao, Y. Wan, Y.Q. Dou, D.Y. Zhao, *Adv. Mater.* 1 (2011) 115–123.